Development and Coil Fabrication Test of the Nb_3Sn Dipole Magnet FRESCA2

P. Manil, B. Baudouy, S. Clément, M. Devaux, M. Durante, P. Fazilleau, P. Ferracin, P. Fessia, J. E. Munoz Garcia, L. Garcia, R. Gauthier, L. Oberli, J. C. Perez, S. Pietrowicz, J. M. Rifflet, G. de Rijk, F. Rondeaux, and E. Todesco

***Abstract*—The key objective of the High Field Magnet work package of the European Project EuCARD is to design and fabricate the Nb_3Sn dipole magnet FRESCA2. It has an aperture of 100 mm and a target bore field of 13 T. The design features four 1.5 m long double-layer coils wound with a 21 mm wide cable. The project has now entered its experimental phase in view of the magnet fabrication. We present the experimental test campaign conducted on cable samples in order to understand and to control better the cable behavior and geometry. One full scale double-layer coil using copper cable with the final dimensions and insulation scheme has been wound and heat treated in order to check the fabrication process. This has given useful feedback on the fabrication procedure and on the expected magnet dimensions, as well as on the tooling itself.**

***Index Terms*—Dipole magnet, EuCARD, FRESCA2, Nb_3Sn, superconducting magnet, winding test.**

I. Introduction

THE European Coordination for Accelerator R&D (EuCARD) project was initiated in 2009 with the goal of carrying out research on new concepts and technologies for future upgrades of the European accelerators [1]. Among its activities, the Work Package 7 is dedicated to superconducting high field magnets for higher luminosities and energies. This work package has as key objective the fabrication and test of FRESCA2, a 100 mm aperture dipole generating a bore field of 13 T [2]. The magnet, which will rely on Nb_3Sn superconductors, is aimed at upgrading the CERN cable test facility FRESCA, which uses Nb–Ti superconductors, bringing the bore field from 10 T to 13 T. In addition, it will provide the background field for an HTS insert [3].

The conceptual design of the FRESCA2 magnet and its support structure was reported in [4]. The conductor parameters and performance are given in [5]. The detailed structure parameters and its protection and instrumentation scheme were reported in [6]. A comprehensive design report has been released [7]. The mechanical structure assembly and test are reported in [8]. Heat transfer studies have been addressed in [9].

Manuscript received July 15, 2013; accepted October 9, 2013. Date of publication October 16, 2013; date of current version October 25, 2013. This work was supported in part by the European Commission under the FP7 Research Infrastructures project EuCARD, Grant 227579.

P. Manil, B. Baudouy, M. Devaux, M. Durante, P. Fazilleau, J. M. Rifflet, and F. Rondeaux are with the CEA Saclay, 91191 Gif-sur-Yvette, France (e-mail: pierre.manil@cea.fr).

S. Pietrowicz was with the CEA Saclay, 91191 Gif-sur-Yvette, France.

S. Clément, P. Ferracin, P. Fessia, J. E. Munoz Garcia, L. Garcia, R. Gauthier, L. Oberli, J. C. Perez, G. de Rijk, and E. Todesco are with the CERN, CH-1211 Geneva 23, Switzerland.

Color versions of one or more of the figures in this paper are available online at http://ieeexplore.ieee.org.

Digital Object Identifier 10.1109/TASC.2013.2285879

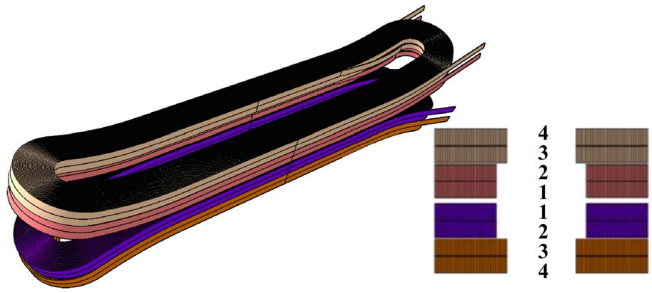

Fig. 1. Geometry of the dipole magnet (without structure). Conductor layers are numbered outwards from 1 to 4. Coils 3–4 are called "outer coils" coils 1–2 are called "inner coils."

The 1.5-m long dipole magnet geometry is represented in Fig. 1. It consists in four flared double-pancake coils of two different types (*inner* and *outer* coils) in block configuration. Each coil is made of one unit Nb_3Sn cable length using either PIT or RRP-type strand. The design of this magnet relies partly on the extensive experience of block coils gained over the years by the LARP collaboration [10]–[15].

This paper summarizes the experimental activities aiming at understanding better the cable behavior and at gaining experience on coils fabrication. The fabrication process is described and the results from the first full-scale prototype coil fabrication, using copper cable, are given.

II. Fabrication Process

A. Cable Fabrication

FRESCA2 cable is a 20.9 mm-wide rectangular Rutherford-type cable, consisting of 40 strands with a diameter of 1.0 mm, obtained from the industry (Bruker-EAS for PIT and OST for RRP strands). The cable is fabricated at CERN with a controlled section that has been defined in order to reduce the critical current degradation [6]. Its thickness of 1.82 mm is controlled periodically in-line under a pressure of 20 MPa.

The cable insulation is braided in-line around it. It consists in continuous S-2 fiberglass yarns that are twisted together to provide strand integrity. These yarns consist themselves in numerous filaments twisted together. A chemical sizing (silane) protects the glass filaments from abrasion during processing. It is removed after operation to avoid any organic pollution during heat treatment. The fabric is treated with a resin-compatible

TABLE I
GEOMETRICAL CHANGES OF THE CABLE DURING REACTION

Direction	PIT cable	RRP cable	Insulation
Cable width	+ 4% *	+ 4% *	0
Cable thickness	+ 2% *	+ 2% *	0
Longitudinal	- 1%	- 0.3%	-

*Values assumed from experience. Other values derive from experimental measurements (see Section III).

finish. FRESCA2 uses 66 tex yarns, referring to the weight (in grams) of 1000 m of fiber.

B. Coil Fabrication

The coil fabrication process follows several stages: winding (with unreacted cable), heat treatment (or reaction), instrumentation, splicing, and impregnation with epoxy resin. Each single double-pancake is fabricated individually. The challenges concerning the design and fabrication of the coil tooling have been reported in [5]. They are related to the high geometrical precision ($\pm$0.05 mm) requested for components up to 1.5 m long, the need of using the same coil parts from winding to magnet assembly, and the high temperature during reaction, which causes differential dilatation and metallurgic changes in the components (see Section III).

Winding is performed on a tailored table specifically designed for one type of double-pancake coil (*inner* or *outer*) and composed of three stainless steel blocks bolted together. To ensure its geometrical stability after reaction, the blocks have undergone a treatment at 930 °C before manufacturing. Machining was finished after assembly of the blocks.

The winding table is mounted on a winding machine allowing rotation and tilt. The top layer (i.e., 2 or 4) is wound first, starting from the layer jump splice. Clamps are used to keep the winding close to its target dimensions. The interlayer insulation layer is put in place and adjusted by hand. The second layer (i.e., 1 or 3) is wound on top of it.

Most of the winding tooling parts are used during reaction. Top plates and lateral shims are added around the coil in order to form a cavity. Its volume is defined according to the dimensions of the cable and their expected variations during heat treatment. As experimental data on FRESCA2 cables was not available at that stage of the project, growth rate values have been assumed when necessary from the experience of previous projects [10]–[13]. They are given in Table I.

Mica sheets are introduced between coil and plates to allow sliding during reaction. After heat treatment (around ten days), the surrounding plates are removed. Instrumentation is put in place on the external faces of the double pancake. It consists in tailor-made printed circuits called "traces" that are connected by hand to the voltage taps [7]. The Nb_3Sn current leads are connected electrically to Nb–Ti cables using 250 W electrical heaters and stabilizing copper parts.

The reaction mold is then replaced by the impregnation mold, made of aluminum and sealed. Heating plates and thermocouples are used to control the impregnation temperature of 110 °C in a vacuum tank at 10^{-1} mbar. The whole tooling is put at an angle of 15° and the appropriate mix of epoxy resin and hardener is injected from the bottom. The curing cycle is done afterwards at 125 °C.

TABLE II
THICKNESS MEASUREMENT OF COPPER TEN-STACKS

Stack number	Insulated cable thickness (mm)	Bare cable thickness (mm)	Insulation thickness (μm)
Copper cable "Cu636S2"			
#1 (Unreacted)	2.259	1.827	216
#2 (Unreacted)	2.255	-	-
#2 (Reacted)	2.257	1.829	214
Copper cable "CuH04UCO107B"			
#1' (Unreacted)	2.237	1.834	201
#2' (Unreacted)	2.238	1.835	201
#3' (Unreacted)	2.240	1.837	202

Each impregnated coil comes out of the impregnation mold as a solid piece that can be assembled with the other coils inside of the magnet structure. The interfaces between coils and structure are done with tailored fiberglass and epoxy resin sheets that are formed using the coils themselves as a mold.

III. CABLE CHARACTERIZATION

A. Measurements on Copper Cable Stacks

For computation and detailed design purposes, the evolution of the bare cable and insulation dimensions along the successive phases of the magnet lifecycle should be known, from coil winding to cool-down and operation at 1.9 K.

To this end, insulated cable samples representative of the different phases are needed: a) unreacted cables representing the winding phase; b) reacted cables representing the heat-treated coil and c) reacted and impregnated cables representing the impregnated coil. The first characterization tests presented here have been done using copper cable with the FRESCA2 dimensions.

To limit experimental errors, the dimensional measurements are performed on stacks of ten conductors. Their fabrication process is representative of the coils' one. The measurement consists in three compression tests with an average pressure of 5 MPa, applied to the large face of the cable. After calibration, the variations in height are recorded and averaged.

In order to study the influence of heat treatment on the insulation, two ten-stacks were prepared using "Cu636S2" copper cable insulated with S2 glass (66 tex, 636 sizing, 100% coverage). The insulation from one ten-stack was removed, and it was measured bare. The insulated ten-stack was heat treated during 5 h at 650 °C. It was then measured and its insulation removed. The insulation thickness indicated on Table II is obtained by difference. This study shows: a) good reproducibility of the thickness values; b) as expected, copper cable thickness is hardly affected by heat treatment; c) heat treatment does not affect the insulation thickness.

A second campaign was led on three ten-stacks using "CuH04UCO107B" copper cable insulated with another S2 glass (66 tex, 936 sizing, 100% coverage), with the same procedure. Results are shown in Table II. The insulation thickness is very close to the initial target 200 μm. This study shows: a) insulation thickness can be precisely controlled; b) the bare copper cable is $\sim$1% thicker than the expected 1.82 mm. The possibility to reduce the insulation thickness

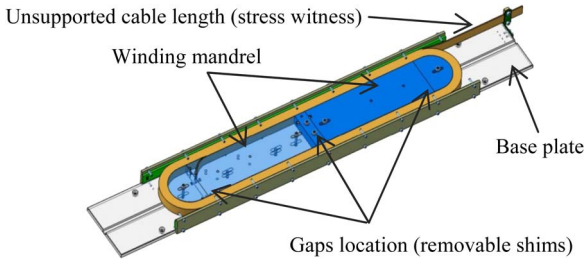

Fig. 2. CAD view of the reaction test fixture.

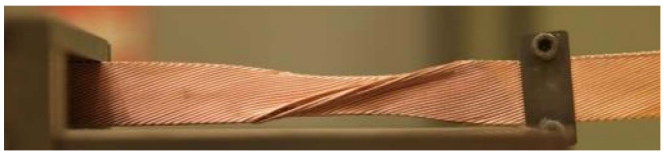

Fig. 3. Unsupported cable end collapsed due to the tension generated during heat treatment without gaps in the mandrel.

is under investigation. As explained in Section IV, the target insulation thickness has later been reduced to 160 μm, which doesn't affect the conclusions of this study.

B. *Effect of Heat Treatment on Nb_3Sn Cable*

As learned from previous projects, the Nb_3Sn cable section expands during heat treatment [10]–[16]. There are additional phenomena at stake, such as winding tension relaxation and metallurgic effects like strand annealing (with relaxation of the residual fabrication stresses) and bronze phase formation. As a result, Nb_3Sn cable tends to contract in length during heat treatment. If the winding and reaction tooling does not allow for longitudinal contraction, tensile stress appears inside of the cable. Current transport properties can be degraded then.

In order to investigate the longitudinal contraction of the cable during heat treatment, a dedicated tooling has been designed. It is represented on Fig. 2. It allows a few conductor turns over one layer, in different configurations.

The winding mandrel is about 700 mm long and 90 mm wide. It is split at several locations by removable shims so that longitudinal gaps can be opened, leading to a few possible configurations: a) a solid one-block mandrel without gaps; b) a segmented mandrel with up to three longitudinal gaps (central/lateral). Split mandrels have already been used successfully by the LARP collaboration [13]. During heat treatment, the mandrel can be either fixed to the base plate or left free. The lead end of the winding consists in a 200 mm long unsupported cable length which serves as a witness of stress. Magnetic steel and titanium alloy mandrels have been used, corresponding to the materials of both central posts [5].

Both PIT and RRP-type cables have been tested, using the relevant thermal cycle. In both cases, the unsupported cable length collapses due to tension when no gap is opened in the mandrel (Fig. 3). This situation is not acceptable for the final magnet. Hence, it is necessary to implement longitudinal gaps in the mandrels. It can be noted that the titanium alloy mandrels leads to reduced deformation compared to steel, which is certainly linked to its lower thermal dilatation.

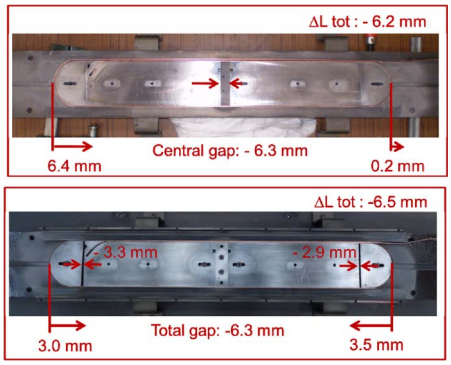

Fig. 4. Two gap configurations for dilatation tests using PIT cable: one central gap (top); two lateral gaps (bottom). Overall contraction (ΔL) is similar.

With one or several gaps, the winding contracts and the unsupported cable piece length shows less deformation. The overall contraction is measured with good reproducibility from one test to the other. As shown on Fig. 4, it is almost independent from the location of the gaps and from the number of turns, which confirms that it is not a local phenomenon. No major difference is observed with respect to the mandrel material.

PIT cable contracts longitudinally by around 1% during heat treatment, while RRP cable contracts by only 0.3%.

This experimental campaign leads to the following conclusions: a) the material of the central posts can be chosen independently from the dilatation issue; b) longitudinal gaps must be implemented in the central posts and in the coil fabrication tooling in order to limit tension on the cable; c) PIT cable contracts longitudinally three times more than RRP cable. Additionally, it is beneficial to add mica sheets around the coil in the reaction tooling so that it can slide easily.

IV. Full-Scale Copper Prototype Fabrication

The *outer* type of coil, called 3–4 because it comprises layers 3 and 4 (see Fig. 1), has been selected for the full-scale prototype because of its larger number of turns and its smaller bending radius compared to coil 1–2. The prototype has been fabricated at CEA-Saclay using "CuH04UCO107B" copper cable insulated as described in Section II-A.

Because of the larger dimensions of the cable with respect to the nominal ones (see Section III-A) only 40 turns were wound instead of the nominal 42, in order to reach the expected overall dimensions of the coil. This will allow us to perform assembly trials with the nominal coil dimensions. Fig. 5 shows layer 4 after winding completion. Lateral compression rails have been installed and the horseshoes have been positioned in the ends to try closing the mold.

Ten voltage taps have been introduced on each layer along the conductor for the future instrumentation [see Fig. 6(a)]. A 0.5 mm interlayer insulation made of fiberglass fabric impregnated with CTD binder was cut and installed on layer 4 before winding layer 3. Fig. 6(b) shows hat the layers are nicely aligned after 40 turns.

Dimensional control has been performed on both layers: measurement of the coil thickness on the two extremities of the straight section and in the ends, showing linear evolution.

Fig. 5. Winding setup after completion of layer 4, showing (*A*) the winding table, (*B*) one horseshoe, and (*C*) the central post.

(a) (b)

Fig. 6. Details of the coil: (a) voltage tap; (b) close-up on the ends.

Dishing and electrical resistance measurements have also been performed. All the results are consistent. They show an average cable thickness of 2.36 $\pm$ 0.01 mm, instead of the 2.22 mm nominal value.

For next coils, this effect will be corrected by reducing the insulation thickness to 160 μm in order to reach the nominal dimensions of the insulated cable while taking into account the assumed section growth as indicated in Table I.

In case of need, the alternative option would be to decrease the number of turns in the coil. It is calculated that the central field of 13 T can be maintained with one turn less, causing 2% reduction of the margin on the load line (81% vs. 79%) [7], [17].

At the end of winding, the reaction mold has been closed around the coil. The coil has been sent to CERN for heat treatment and impregnation.

V. Consequences on the Tooling

Fabrication of the full-scale copper prototype has allowed validating the tooling design and the winding procedure. Minor changes have been proposed by the fabrication team in order to improve the tooling ergonomics before manufacturing the final coils. A prototype *inner* coil (called 1–2 because it comprises layers 1 and 2) will be fabricated using copper cable to check the second set of tooling.

Following the conclusions from Section III-B, the tooling must now be adapted for Nb_3Sn coils fabrication. The experimental tests have shown that opening longitudinal gaps in the winding table and in the central post is necessary in order to handle the cable contraction during heat treatment and to avoid any cable degradation. The final coils geometry must be controlled, because they have to be assembled together, even if they are made from different type of Nb_3Sn cable. Hence, it has been decided to define the thickness of the gaps so that they just close during reaction, with reduced tension. From the figures given in Table I, it would lead to approximately 15 mm (5 mm) gaps for PIT (RRP) cable, spread between the straight section and probably the ends. It is planned to benefit from the interfaces existing between the winding table blocks. It also means that the central post and the insulation layers will have to be split at the same location.

VI. Conclusion

In this paper, the successful fabrication of the first copper full-scale prototype coil for FRESCA2 has been reported. This test has helped to verify the practical feasibility of our design and to choose between technical options. Experimental test campaign has helped to understand the behavior of Nb_3Sn conductor during high temperature heat treatment and operation. Mechanical and assembly tests have been performed to validate the mechanical structure of the magnet.

Along the study, technological difficulties have emerged due to the longitudinal contraction of the Nb_3Sn cable during heat treatment that needed to be quantified. They have led to additional analysis and tests, which are described in this document.

In a near future, the winding tooling will be adapted to the conductor behavior during reaction. Two first Nb_3Sn coils will be assembled with two copper prototype coils to form a magnet that will be inserted in the mechanical support structure. After cold test of this magnet, two other Nb_3Sn coils will be fabricated to form the final FRESCA2 magnet, which will be cold-tested and qualified.

Acknowledgment

The authors wish to acknowledge all people who participated in this study at CERN and at CEA-Saclay: people from the design office and the workshops, and also all the colleagues who provided us with useful ideas and comments along this project.

We would like to stress the essential and constructive role of the External Scientific Advisory Committee members in guiding and advising wisely our decisions.

References

[1] [Online]. Available: http://eucard.web.cern.ch
[2] G. de Rijk, "The EuCARD high field magnet project," *IEEE Trans. Appl. Supercond.*, vol. 22, no. 3, p. 4301294, Jun. 2012.
[3] J.-M. G. Rey *et al.*, "HTS dipole insert development," *IEEE Trans. Appl. Supercond.*, vol. 23, no. 3, p. 4601004, Jun. 2013.
[4] A. Milanese, M. Devaux, M. Durante, P. Manil, J. C. Perez, J. M. Rifflet, G. de Rijk, and F. Rondeaux, "Design of the EuCARD high field model dipole magnet FRESCA2," *IEEE Trans. Appl. Supercond.*, vol. 22, no. 3, p. 4002604, Jun. 2012.

[5] P. Ferracin, M. Devaux, M. Durante, P. Fazilleau, P. Fessia, P. Manil, A. Milanese, J. E. Munoz Garcia, L. Oberli, J. C. Perez, J. M. Rifflet, G. de Rijk, F. Rondeaux, and E. Todesco, "Development of the EuCARD Nb_3Sn dipole magnet FRESCA2," *IEEE Trans. Appl. Supercond.*, vol. 23, no. 3, p. 4002005, Jun. 2013.

[6] L. Oberli, "Development of the Nb_3Sn rutherford cable for the EuCARD high field dipole magnet FRESCA2," *IEEE Trans. Appl. Supercond.*, vol. 23, no. 3, p. 4800704, Jun. 2013.

[7] P. Manil *et al.*, "Dipole model test with one superconducting coil, results analyzed—Part I: Design report for the dipole magnet," May 2013, EuCARD deliverable D7.3.1.a-v1.0.

[8] J. E. Muñoz Garcia, C. Giloux, D. Ziemiansk, F. Rondeaux, G. DeRijk, H. Bajas, J. Rifflet, J. Perez, M. Durante, M. Charrondiere, M. Bajko, M. Devaux, M. Guinchard, P. Ferracin, P. Fessia, and P. Manil, "Assembly, loading, cool-down of the FRESCA2 support structure," *IEEE Trans. Appl. Supercond.*, to be published.

[9] S. Pietrowicz and B. Baudouy, "Numerical study of the thermal behavior of an Nb_3Sn high field magnet in He II," *Cryogenics*, vol. 53, pp. 72–77, Jan. 2013.

[10] H. Felice, G. Ambrosio, M. D. Anerella, D. Bocian, R. Bossert, S. Caspi, B. Collins, D. Cheng, G. Chlachidze, D. R. Dietderich, P. Ferracin, A. Godeke, A. Ghosh, A. R. Hafalia, J. M. Joseph, J. Krishnan, M. Marchevsky, G. Sabbi, J. Schmalzle, P. Wanderer, X. R. Wang, and A. Zlobin, "Impact of coil compaction on Nb_3Sn LARP HQ magnet," *IEEE Trans. Appl. Supercond.*, vol. 22, no. 3, p. 4001904, Jun. 2012.

[11] P. Ferracin, B. Bingham, S. Caspi, D. W. Cheng, D. R. Dietderich, H. Felice, A. R. Hafalia, C. R. Hannaford, J. Joseph, A. F. Lietzke, J. Lizarazo, G. Sabbi, and X. Wang, "Recent test results of the high field Nb_3Sn dipole magnet HD2," *IEEE Trans. Appl. Supercond.*, vol. 20, no. 3, pp. 292–295, Jun. 2010.

[12] G. Ambrosio, N. Andreev, M. Anerella, E. Barzi, B. Bingham, D. Bocian, R. Bossert, S. Caspi, G. Chlachidize, D. Dietderich, J. Escallier, H. Felice, P. Ferracin, A. Ghosh, A. Godeke, R. Hafalia, R. Hannaford, G. Jochen, V. V. Kashikhin, M. J. Kim, P. Kovach, M. Lamm, A. McInturff, J. Muratore, F. Nobrega, I. Novitsky, D. Orris, E. Prebys, S. Prestemon, G. L. Sabbi, J. Schmalzle, C. Sylvester, M. Tartaglia, D. Turrioni, G. Velev, P. Wanderer, G. Whitson, and A. V. Zlobin, "Test results of the first 3.7 m long Nb_3Sn quadrupole by LARP and future plans," *IEEE Trans. Appl. Supercond.*, vol. 21, no. 3, pp. 1858–1862, Jun. 2011.

[13] G. Ambrosio, N. Andreev, M. Anerella, E. Barzi, R. Bossert, S. Caspi, G. Chlachidize, D. R. Dietderich, H. Felice, P. Ferracin, A. Ghosh, R. Hafalia, R. Hannaford, G. Jochen, V. V. Kashikhin, P. Kovach, M. Lamm, A. Lietzke, A. D. McInturff, J. F. Muratore, F. Nobrega, I. Novitsky, S. Peggs, S. Prestemon, G. L. Sabbi, J. Schmalzle, D. Turrioni, P. Wanderer, G. Whitson, and A. V. Zlobin, "Development and coil fabrication for the LARP 3.7-m long Nb_3Sn quadrupole," *IEEE Trans. Appl. Supercond.*, vol. 19, no. 3, pp. 1231–1234, Jun. 2009.

[14] G. Ambrosio, N. Andreev, M. Anerella, E. Barzi, B. Bingham, D. Bocian, B. Bordini, R. Bossert, L. Bottura, S. Caspi, G. Chlachidize, W. M. de Rapper, D. Dietderich, J. Escallier, H. Felice, P. Ferracin, A. Ghosh, A. Godeke, R. Hafalia, R. Hannaford, G. Jochen, V. V. Kashikhin, P. Kovach, M. Lamm, A. McInturff, J. Muratore, F. Nobrega, I. Novitsky, D. Orris, S. Peggs, E. Prebys, S. Prestemon, G. L. Sabbi, J. Schmalzle, C. Sylvester, M. Tartaglia, D. Turrioni, G. Velev, P. Wanderer, G. Whitson, G. Willering, and A. V. Zlobin, "Final development and test preparation of the first 3.7 m long Nb_3Sn quadrupole by LARP," *IEEE Trans. Appl. Supercond.*, vol. 20, no. 3, pp. 283–287, Jun. 2010.

[15] D. W. Cheng, S. Caspi, D. R. Dietderich, H. Felice, P. Ferracin, A. R. Hafalia, M. Marchevsky, S. Prestemon, and G. Sabbi, "Design and fabrication experience with Nb_3Sn block-type coils for high field accelerator dipoles," *IEEE Trans. Appl. Supercond.*, vol. 23, no. 3, p. 4002504, Jun. 2013.

[16] E. Fornasiere, H. Bajas, M. Bajko, B. Bordini, S. Canfer, G. Ellwood, P. Ferracin, P. Fessia, J. Feuvrier, M. Guinchard, C. Kokkinos, P. Manil, A. Milanese, L. Oberli, J. C. Perez, and G. de Rijk, "Status of the activities on the Nb_3Sn dipole SMC and of the design of the RMC," *IEEE Trans. Appl. Supercond.*, vol. 23, no. 3, p. 4002308, Jun. 2013.

[17] M. Devaux, "Internal calculation note," CEA-Saclay, Dec. 2012.